Available online at www.sciencedirect.com
SCIENCE DIRECT®
ELSEVIER
Journal of Sound and Vibration 275 (2004) 47–57
JOURNAL OF SOUND AND VIBRATION
www.elsevier.com/locate/jsvi

Transverse vibration of an uniform Euler–Bernoulli beam under linearly varying axial force

S. Naguleswaran*

Department of Mechanical Engineering, University of Canterbury, Christchurch 8020, New Zealand

Received 13 August 2002; accepted 24 June 2003

Abstract

This paper is concerned with the transverse vibration of uniform Euler–Bernoulli beams under linearly varying fully tensile, partly tensile or fully compressive axial force distribution. The system parameters are the constant part of the axial force and the constant of proportionality of the varying part. The mode shape differential equation is linear with variable coefficients. The general solution is derived and expressed as the super-position of four independent power series solution functions. The frequency equations of the 16 combinations of classical boundary conditions are listed. The first three frequency parameters are tabulated for example combinations of the system parameters. Increase in the values of one or both of the system parameters 'stiffens' the system and results in increase in the frequency parameter. If one or both system parameters are negative, combinations exist for which a frequency parameter is zero. This is the Euler buckling condition i.e., onset of dynamic instability. Example combinations of the system parameters when buckling occurs are tabulated. The results tabulated may be used to judge frequencies, buckling parameter combinations obtained by other methods.
© 2003 Elsevier Ltd. All rights reserved.

1. Introduction

Structural elements, components of mechanisms and the like are often subjected to axially distributed force. For example a tie-bar is under a constant axial force, a vertically oriented uniform beam in a gravity field is subjected to a linearly distributed axial force and a beam in a centrifugal field to a parabolic distribution. The transverse vibration of uniform tie-bars is discussed in textbooks [1]. Bokian [2] presented (in graphical form), the frequencies of a uniform

*Tel.: +64-3-364-2987; fax: +64-3-364-2078.
E-mail address: s.naguleswaran@mech.canterbury.ac.nz (S. Naguleswaran).

0022-460X/$ - see front matter © 2003 Elsevier Ltd. All rights reserved.
doi:10.1016/S0022-460X(03)00741-7

beam under constant axial compressive force. Bokian [3] extended the work in Ref. [2] to a uniform tie-bar for 10 combinations of classical boundary conditions.

Paidoussis and Des Trois Maissons [4] used the Galerkin method to study the transverse vibration of 'hanging' and 'standing' uniform cantilevers taking account of the self-weight. Schafer [5] used the Rayleigh–Ritz method to investigate the same problem. Fauconneau and Laird [6] used the Rayleigh–Ritz method (with 8 sinusoidal terms in the Ritz manifold) to obtain upper bound frequencies of a simply supported uniform beam under a linearly distributed axial force. A method to obtain lower bounds was described. Approximate frequencies obtained by replacing the distributed load by a 'lumped' axial force were included. In the absence of 'exact' solution, no comments were offered on the 'error' estimates. Pilkington and Carr [7] used a method based on the results of static buckling to obtain 'lower' bound frequencies for the problem in Ref. [6]. Yokoyama [8] used the finite element method to study the vibration of 'hanging' Timoshenko and Euler–Bernoulli uniform cantilevers.

The mode shape differential equation of uniform Euler–Bernoulli beams under linearly varying axial force was derived in Refs. [5–8] and because it had variable coefficients these references concluded that analytical solution was 'difficult or impossible'. The mode shape differential equation is linear and this aspect appears to have been overlooked. Naguleswaran [9] solved the mode shape differential equation of a 'hanging' uniform cantilever by the method of Frobenius [10]. The general solution consisted of the super-position of four linearly independent power series solution functions. The frequency equation for ideal clamped–free boundary conditions was formulated. The first three natural frequencies of uniform cantilevers were tabulated for positive and negative values of the gravity parameter (a measure of gravity effect over flexural rigidity effect).

In the present paper a more general case is considered. The axial tension distribution consisted of a constant part and a part proportional to the axial co-ordinate. These are the two system parameters. The mode shape equation is solved and frequency equations of all the 16 combinations of classical boundary conditions are listed. Wholly tensile, partly tensile and wholly compressive axial force distribution is considered.

Buckling under self-weight of a vertical cantilever was investigated as a problem in statics by Greenhill [11] and by Frish-Fay [12] and the first critical gravity parameter was presented in terms of Bessel's functions. Naguleswaran [9] approached the problem as the limiting case at which a natural frequency is zero and listed the first three critical gravity parameters of a 'standing' cantilever. Gooch and Raine [13] used the low frequencies near buckling condition of a 'standing' cantilever to design a scaled version of the Len Lye kinetic sculpture *Blade* noted for the aesthetic performance. In the present paper example combinations of the system parameters for which a natural frequency is zero (dynamic instability or buckling) are tabulated for 16 combinations of classical boundary conditions.

The results tabulated in the present paper are not found in any other publications. The results may be used to judge frequencies or buckling parameter combinations obtained by other methods.

2. Theory

The flexural rigidity, mass per unit length and length of the uniform Euler–Bernoulli beam OA considered in this paper are EI, m and L respectively (see Fig. 1). The end O is axially restrained

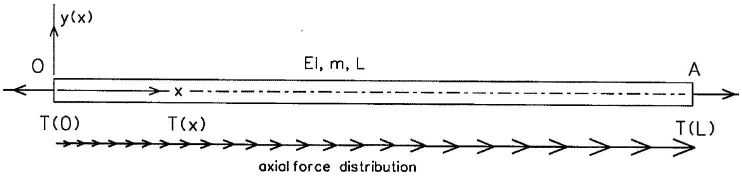

Fig. 1. The beam, co-ordinate system and the axial force distribution. The end O is axially restrained and A is axially free.

while A is axially free. The origin of the co-ordinate system chosen is at O with the abscissa along the neutral axis of the beam. $T(0)$ and $T(L)$ are the axial force at O and A respectively. The linear axial force distribution $T(x)$ at abscissa x is

$$T(x) = T(0) + [T(L) - T(0)]\,\frac{x}{L}. \tag{1}$$

Positive axial force is tensile and negative axial force is compressive.

For free vibration at frequency ω, if at abscissa $x, y(x)$ is the amplitude of deflection of the beam, $M(x)$ and $Q(x)$ are the amplitudes of bending moment and shearing force, then consideration of the equilibrium of a differential element [1] will lead to

$$M(x) = EI\frac{\mathrm{d}^2y(x)}{\mathrm{d}x^2}, \quad Q(x) + \frac{\mathrm{d}M(x)}{\mathrm{d}x} - T(x)\frac{\mathrm{d}y(x)}{\mathrm{d}x} = 0, \quad \frac{\mathrm{d}Q(x)}{\mathrm{d}x} + m\omega^2y(x) = 0. \tag{2}$$

Introduce the dimensionless variables X, $Y(X)$, operators D^n, bending moment $M(X)$, shearing force $Q(X)$, axial force $\tau(X)$, constant axial force parameter τ_0, the variable axial force parameter γ, frequency parameter α defined as follows:

$$\begin{aligned}
&X = \frac{x}{L}, \quad Y(X) = \frac{y(x)}{L}, \quad D^n = \frac{\mathrm{d}^n}{\mathrm{d}X^n},\\
&M(X) = \frac{M(x)L}{EI}, \quad Q(X) = \frac{Q(x)L^2}{EI},\\
&\tau(X) = \frac{T(x)L^2}{EI}, \quad \tau(0) = \frac{T(0)L^2}{EI},\\
&\tau(1) = \frac{T(L)L^2}{EI}, \quad \gamma = \tau(1) - \tau(0), \quad \alpha^4 = \frac{m\omega^2L^4}{EI}.
\end{aligned} \tag{3}$$

Eqs. (1) and (2) in dimensionless form are

$$\begin{aligned}
&\tau(X) = \tau(0) + \gamma X, \quad M(X) = D^2[Y(X)], \quad Q(X) = -D^3[Y(X)] + [\tau(0) + \gamma X]D[Y(X)],\\
&D^4[Y(X)] - \tau(0)D^2[Y(X)] - \gamma D\{XD[Y(X)]\} - \alpha^4 Y(X) = 0.
\end{aligned} \tag{4}$$

The dimensionless mode shape differential Eq. (4) is linear with variable coefficients and may be solved by the method of Frobenius [10]. The power series solution sought is

$$Y(X, c) = \sum_{n=0}^{n=\infty} a_{n+1}(c)X^{c+n} \tag{5}$$

in which the coefficients $a_{n+1}(c)$ are functions of the undetermined exponent c. Without loss of generality the lead coefficient $a_1(c)$ was chosen to be unity. Following the method of Frobenius,

$Y(X, c)$ was substituted into the mode shape differential equation and the coefficients chosen from the recurrence relationship

$$a_{n+2}(c) = \frac{\tau(0)(c+n-1)(c+n-2)a_n(c) + \gamma(c+n-2)^2 a_{n-1}(c) + \alpha^4 a_{n-2}(c)}{(c+n+1)(c+n)(c+n-1)(c+n-2)} \tag{6}$$

subject to $a_k(c) = 0$ if the subscript $k \leqslant 0$. With these choices, $Y(X, c)$ will satisfy the mode shape differential Eq. (4) provided c is a root of the indicial equation

$$c(c-1)(c-2)(c-3) = 0. \tag{7}$$

The four power series solution functions are

$$\begin{aligned}
Y(X,0) = E(X) &= 1 + (0)X + \frac{\tau(0)X^2}{2} + (0)X^3 + \sum_{n=0}^{n=\infty} e_{n+5}X^{n+4},\\
Y(X,1) = F(X) &= X + (0)X^2 + \frac{\tau(0)X^3}{6} + \frac{\gamma X^4}{24} + \sum_{n=0}^{n=\infty} f_{n+5}X^{n+5},\\
Y(X,2) = G(X) &= X^2 + (0)X^3 + \frac{\tau(0)X^4}{12} + \frac{\gamma X^5}{30} + \sum_{n=0}^{n=\infty} g_{n+5}X^{n+6},\\
Y(X,3) = H(X) &= X^3 + (0)X^4 + \frac{\tau(0)X^5}{20} + \frac{\gamma X^6}{40} + \sum_{n=0}^{n=\infty} h_{n+5}X^{n+7}.
\end{aligned} \tag{8}$$

The coefficients of the solution functions are

$$\begin{aligned}
e_{n+1} &= a_{n+1}(0), \quad f_{n+1} = a_{n+1}(1),\\
g_{n+1} &= a_{n+1}(2), \quad h_{n+1} = a_{n+1}(3).
\end{aligned} \tag{9}$$

The derivatives of the solution functions may be obtained on a term by term basis. The general solution of the mode shape differential equation is

$$Y(X) = C_1E(X) + C_2F(X) + C_3G(X) + C_4H(X) \tag{10}$$

in which C_1, C_2, C_3 and C_4 are constants of integration.

2.1. The frequency equations

The boundary conditions at O may be utilized to eliminate two of the constants of integration in Eq. (10) and the mode shape expressed as

$$Y(X) = AU(X) + BV(X), \tag{11}$$

where A and B are constants and the functions $U(X)$ and $V(X)$ for the classical clamped (*cl*), pinned (*pn*), sliding (*sl*) or free (*fr*) boundary conditions are

$$\begin{aligned}
O\ cl: &\quad U(X) = G(X),\ V(X) = H(X),\\
O\ pn: &\quad U(X) = F(X),\ V(X) = H(X),\\
O\ sl: &\quad U(X) = E(X),\ V(X) = G(X),\\
O\ fr: &\quad U(X) = E(X) - 0.5\tau(0)G(X),\ V(X) = F(X).
\end{aligned} \tag{12}$$

Clamped, pinned and sliding boundary condition at O require two of the four solution functions and free boundary condition require three functions. Had the support at O been resilient, all the four functions will appear in the mode shape equation.

The mode shape Eq. (11) must satisfy the boundary conditions at A. The frequency equation for the four classical boundary conditions at A are

$$\begin{aligned} A\ cl: &\quad U(1)D[V(1)] - D[U(1)]V(1) = 0 \\ A\ pn: &\quad U(1)D^2[V(1)] - D^2[U(1)]V(1) = 0 \\ A\ sl: &\quad D[U(1)]D^3[V(1)] - D^3[U(1)]D[V(1)] = 0 \\ A\ fr: &\quad D^2[U(1)]\{D^3[V(1)] - \tau(1)D[V(1)]\} - \{D^3[U(1)] - \tau(1)D[U(1)]\}D^2[V(1)] = 0 \end{aligned} \tag{13}$$

The natural frequencies of the selected system will be obtained from the roots of the corresponding frequency equation. All the 16 frequency equations are considered in this paper.

2.2. 'Equivalent' $\tau(0)$ and γ pairs

The axial force distribution $\tau(X) = \tau(0) + \gamma - \gamma X$ is a mirror image of $\tau(X) = \tau(0) + \gamma X$. If the boundary conditions at O and A are denoted by (i,j) where i or $j = 1, 2, 3$ or 4 respectively stand for *cl*, *pn*, *sl* or *fr* boundary conditions and if the nth frequency parameter corresponding to the system parameters $\tau(0)$ and γ is denoted by $\alpha_n(i,j,\tau(0),\gamma)$ then

$$\alpha_n(i,\ j,\ \tau(0),\ \gamma) = \alpha(j,\ i,\ \tau(0) + \gamma,\ -\gamma). \tag{14}$$

2.3. Natural frequency parameter calculations

The solution functions applicable to the boundary conditions at O were chosen from the equation set (12). For the selected set of the system parameters $\tau(0)$ and γ and an assumed value for α, sufficient number of terms were allowed so that at $X = 1.0$, the functions and their derivatives converged to a pre-set accuracy range. The frequency equation corresponding to the boundary conditions at A was now chosen from the equation set (13). Starting with a trial value of $\alpha = 0.1$ the left side of the frequency equation was evaluated. Calculations were repeated with step increase of 0.1 in α till a sign change was observed. This indicates a 'range' in which a root lies. Calculations were repeated in this 'range' with step change of 0.01 in α to narrow the 'range'. An iterative procedure based on linear interpolation was invoked to calculate the root to a pre-set accuracy. The search was continued for the second root and so on.

Rigid body translation is possible for *sl−sl*, *sl−fr* and *fr−sl* systems. Rigid body translation and rotation is possible for *fr−fr* system. The frequency equations of *sl−sl*, *sl−fr*, *fr−sl* and *fr−fr* will have zero as the first root. The first three non-zero frequency parameters for nine example combinations of $\tau(0)$ and γ are tabulated in Tables 1–3 as three 3-column sets. Calculations were in double precision. It was found that for $\gamma > 800$, computation in quadruple precision was required and for $\gamma > 1000$ greater computing precision was required.

In Table 1 the frequency parameters α_1, α_2 and α_3 are tabulated for system parameter combinations $[\tau(0), \gamma] = (10, 100), (10, 4)$ and $(10, -3)$. For these example combinations of $[\tau(0), \gamma]$, in the range $0 \leqslant X \leqslant 1$ the axial force $T(X)$ is tensile. Increase in $\tau(0)$ and/or γ 'stiffens' the beam

Table 1
The first three frequency parameters for $\tau(0) = 10.0$ and γ as stated in first row

BC	$\gamma = 100.0$			$\gamma = 4.0$			$\gamma = -3.0$		
	α_1	α_2	α_3	α_1	α_2	α_3	α_1	α_2	α_3
cl\cl	5.8768	8.9720	11.9595	5.0437	8.1234	11.2122	4.9587	8.0475	11.1503
cl\pn	5.5709	8.5122	11.3932	4.4144	7.4147	10.4694	4.2647	7.3077	10.3898
cl\sl	3.5912	7.0372	9.9341	2.8569	5.9054	8.9358	2.7525	5.7828	8.8455
cl\fr	3.5876	6.9736	9.7435	2.7660	5.4542	8.3161	2.5956	5.2063	8.1548
pn\cl	5.2505	8.2814	11.2405	4.3835	7.4000	10.4614	4.2906	7.3192	10.3960
pn\pn	5.0032	7.8617	10.6990	3.8322	6.7141	9.7281	3.6689	6.5970	9.6426
pn\sl	3.0737	6.4101	9.2566	2.4084	5.2461	8.2099	2.3111	5.1127	8.1122
pn\fr	3.0722	6.3678	9.1013	2.3588	4.8738	7.6238	2.2170	4.6126	7.4454
sl\cl	3.8567	6.8370	9.7732	2.8713	5.8892	8.9265	2.7415	5.7959	8.8526
sl\pn	3.7150	6.5037	9.2877	2.4770	5.2530	8.2117	2.2478	5.1071	8.1108
sl\sl	5.0483	7.8632	10.6986	3.8325	6.7141	9.7281	3.6691	6.5970	9.6426
sl\fr	5.0346	7.7720	10.4718	3.6296	6.2133	9.0873	3.3514	5.9897	8.9404
fr\cl	3.7806	6.3957	9.1596	2.7547	5.3778	8.2704	2.6142	5.2739	8.1912
fr\pn	3.6551	6.1204	8.7159	2.4090	4.8209	7.5858	2.1752	4.6632	7.4765
fr\sl	4.8344	7.3614	10.0767	3.5792	6.1613	9.0567	3.4052	6.0345	8.9647
fr\fr	4.8247	7.2942	9.8855	3.4222	5.7311	8.4498	3.1479	5.4969	8.2900

Table 2
The first three frequency parameters for $\tau(0) = 0.0$ and γ as stated in first row

BC	$\gamma = 100.0$			$\gamma = 4.0$			$\gamma = -3.0$		
O\A	α_1	α_2	α_3	α_1	α_2	α_3	α_1	α_2	α_3
cl\cl	5.7250	8.8109	11.8130	4.7869	7.9002	11.0326	4.6857	7.8173	10.9676
cl\pn	5.4086	8.3359	11.2317	4.0397	7.1368	10.2583	3.8332	7.0159	10.1736
cl\sl	3.4351	6.8590	9.7630	2.4649	5.5806	8.6951	2.2772	5.4327	8.5968
cl\fr	3.4311	6.7878	9.5543	2.1943	4.9046	7.9602	1.1784	4.5088	7.7723
pn\cl	5.0321	8.0843	11.0709	3.9954	7.1201	10.2498	3.8722	7.0291	10.1801
pn\pn	4.7784	7.6485	10.5129	3.2884	6.3611	9.4773	3.0136	6.2225	9.3847
pn\sl	2.8104	6.1822	9.0552	1.7298	4.8102	7.9158	1.4001	4.6342	7.8065
pn\fr	2.8091	6.1357	8.8846	1.5007	4.1880	7.1912	*uns*	3.6762	6.9714
sl\cl	3.7161	6.6309	9.5907	2.4799	5.5604	8.6850	2.2661	5.4492	8.6046
sl\pn	3.5779	6.2861	9.0884	1.8972	4.8191	7.9178	0.9580	4.6266	7.8050
sl\sl	4.8353	7.6496	10.5123	3.2890	6.3611	9.4773	3.0140	6.2225	9.3847
sl\fr	4.8206	7.5489	10.2658	2.8152	5.6715	8.7340	1.4611	5.3530	8.5659
fr\cl	3.5873	6.0423	8.8871	2.0777	4.7755	7.9057	1.6627	4.6300	7.8158
fr\pn	3.4756	5.7639	8.4230	1.5634	4.0703	7.1423	*uns*	3.8066	7.0116
fr\sl	4.5067	7.0264	9.8161	2.6194	5.5920	8.6981	2.0979	5.4235	8.5944
fr\fr	4.4981	6.9550	9.6082	2.1771	4.9449	7.9629	*uns*	4.5420	7.7672

uns, unstable mode.

Table 3
The first three frequency parameters for $\tau(0) = -2.0$ and γ as stated in first row

BC	$\gamma = 100.0$			$\gamma = 4.0$			$\gamma = -3.0$		
O\A	α_1	α_2	α_3	α_1	α_2	α_3	α_1	α_2	α_3
cl\cl	5.6930	8.7775	11.7830	4.7299	7.8532	10.9956	4.6245	7.7686	10.9299
cl\pn	5.3743	8.2993	11.1986	3.9500	7.0771	10.2145	3.7256	6.9530	10.1286
cl\sl	3.4011	6.8217	9.7277	2.3567	5.5082	8.6445	2.1306	5.3538	8.5444
cl\fr	3.3970	6.7487	9.5150	1.9677	4.7640	7.8827	*uns*	4.3181	7.6886
pn\cl	4.9843	8.0431	11.0361	3.9016	7.0599	10.2058	3.7689	6.9665	10.1353
pn\pn	4.7290	7.6037	10.4745	3.1398	6.2830	9.4247	2.8143	6.1389	9.3305
pn\sl	2.7468	6.1334	9.0133	1.4154	4.7071	7.8529	*uns*	4.5184	7.7409
pn\fr	2.7455	6.0859	8.8392	*uns*	3.9941	7.0939	*uns*	3.3601	6.8637
sl\cl	3.6854	6.5871	9.5529	2.3717	5.4870	8.6342	2.1196	5.3712	8.5523
sl\pn	3.5482	6.2397	9.0469	1.6825	4.7167	7.8549	cc	4.5102	7.7393
sl\sl	4.7889	7.6047	10.4738	3.1405	6.2830	9.4247	2.8149	6.1389	9.3305
sl\fr	4.7740	7.5018	10.2230	2.5060	5.5401	8.6577	*uns*	5.1930	8.4847
fr\cl	3.5394	5.9599	8.8292	1.7272	4.6176	7.8261	*uns*	4.4575	7.7337
fr\pn	3.4317	5.6802	8.3603	*uns*	3.8485	7.0424	*uns*	3.5312	6.9060
fr\sl	4.4255	6.9519	9.7613	2.1551	5.4527	8.6206	*uns*	5.2709	8.5141
fr\fr	4.4172	6.8795	9.5496	*uns*	4.7276	7.8529	*uns*	4.2481	7.6479

uns, unstable mode.

and results in an increase in α_n. For *sl−sl*, *sl−fr* and *fr−sl* beams the α_n listed is technically α_{n+1} and for *fr−fr* beams the α_n listed is technically α_{n+2}.

In Table 2, the axial force in the range $0 \leqslant X \leqslant 1$ for the system parameter combinations $[\tau(0), \gamma] = (0, 100)$ and $(0, 4)$ are positive and the comments made for Table 1 are applicable for the first and second 3-column sets. The axial force in the range $0 \leqslant X \leqslant 1$ for $[\tau(0), \gamma] = (0, -3)$ is negative and for this combination, the first mode of *pn−fr*, *fr − pn* and *fr−fr* beams are unstable (the critical values of γ which initiates onset of instability is discussed later).

In Table 3, for the combination $[\tau(0), \gamma] = (-2, 100)$, the axial tension is negative at O and is positive at A and the frequency parameters fit the pattern of the first 3-column sets of Tables 1 and 2. For the combination $[\tau(0), \gamma] = (-2, 4)$ the axial tension is negative at O and positive at A but unlike the first 3-column set, the first mode of *pn−fr*, *fr−pn* and *fr−fr* beams are unstable. For the combination $[\tau(0), \gamma] = (-2, -3)$, the axial tension is negative in the range $0 \leqslant X \leqslant 1$. For this combination of system parameters, *cl−fr*, *pn−sl*, *pn−fr*, *sl−pn*, *sl−fr*, *fr−cl*, *fr−pn*, *fr−sl*, and *fr−fr* are past the first mode Euler buckling.

Faucanneau and Laird [6] presented a table of Rayleigh–Ritz frequencies of *pn−pn* beam for a number of combinations of $[\tau(0), \gamma]$. It was found that these frequencies were upper bounds to the 'exact' frequencies calculated by the present method and in most cases agreement to third places after the decimal point obtained.

2.4. Euler buckling

A decrease in $\tau(0)$ and/or γ results in a decrease in α. For certain combinations of $\tau(0)$ and γ, a frequency parameter may be zero. This is the onset of instability or Euler buckling and further decrease in the system parameter/s will render the particular mode to be unstable. A necessary (but not sufficient) condition for Euler buckling to occur is for part of the beam to be under negative (compressive) axial force.

For a selected combination of boundary conditions and a given value of $\tau(0)$, the nth critical γ (denoted by $\gamma_{c,n}$) must satisfy the corresponding frequency Eq. (13) in which $\alpha = 0$. To calculate the critical $\gamma_{c,n}$, the 'search' followed by the iterative routine used for frequency parameter calculations was used. For the special case $\tau(0) = 0$, rigid body motion is possible for *pn−fr*, *sl−sl*, *sl−fr*, *fr−pn*, *fr−sl* and *fr−fr* boundary conditions and for these cases $\gamma_{c,1} = 0$. In Table 4 $\gamma_{c,1}$ and $\gamma_{c,2}$ pairing with $\tau(0) = 10, 4, 1, 0, -0.5, -1, -2$, and -4 are tabulated for *cl−cl*, *cl−pn*, *cl−sl*, *cl−fr*, *pn−cl*, *pn−pn*, *pn−sl* and *pn−fr* boundary conditions. The other boundary conditions are not listed because

$$\begin{aligned}
&\gamma_{c,n}(sl-cl) = \gamma_{c,n}(cl-sl) = \gamma_{c,n}(sl-sl),\\
&\gamma_{c,n}(sl-pn) = \gamma_{c,n}(cl-fr) = \gamma_{c,n+1}(sl-fr),\\
&\gamma_{c,n}(fr-cl) = \gamma_{c,n}(pn-sl) = \gamma_{c,n}(fr-sl),\\
&\gamma_{c,n}(fr-pn) = \gamma_{c,n}(pn-fn) = \gamma_{c,n+1}(fr-fr).
\end{aligned} \tag{15}$$

For the $[\tau(0), \gamma_c]$ pairs, a decrease in $\tau(0)$ is compensated by a corresponding increase in γ_c. In Table 5, approximate $\gamma_{c,1}$ obtained by Fauconneau and Laird [6] using 8 terms-Rayleigh–Ritz method are compared with 'exact' values obtained by the present method.

Table 4
The first two critical γ_c for various $\tau(0)$

BC	$\tau(0) = 10.0$		$\tau(0) = 4.0$		$\tau(0) = 1.0$		$\tau(0) = 0.0$	
O\A	$\gamma_{c,1}$	$\gamma_{c,2}$	$\gamma_{c,1}$	$\gamma_{c,2}$	$\gamma_{c,1}$	$\gamma_{c,2}$	$\gamma_{c,1}$	$\gamma_{c,2}$
cl\cl	−92.3767	−175.740	−81.7753	−164.538	−76.4214	−158.912	−74.6286	−157.033
cl\pn	−44.3406	−130.246	−35.7783	−119.383	−31.4564	−113.920	−30.0094	−112.095
cl\sl	−36.8379	−102.673	−26.2477	−90.238	−20.7980	−83.978	−18.9562	−81.887
cl\fr	−16.9986	−63.746	−8.9816	−52.050	−4.8670	−46.124	−3.4766	−44.138
pn\cl	−74.9929	−150.759	−61.7249	−137.772	−54.8374	−131.237	−52.5006	−129.054
pn\pn	−35.5755	−108.398	−25.5475	−95.300	−20.3384	−88.657	−18.5687	−86.431
pn\sl	−32.7393	−85.758	−18.8726	−68.036	−10.7718	−58.984	−7.8372	−55.977
pn\fr	−16.2148	−54.020	−7.1718	−37.511	−1.9375	−28.638	cc	−25.638
BC	$\tau(0) = -0.5$		$\tau(0) = -1.0$		$\tau(0) = -2.0$		$\tau(0) = -4.0$	
O\A	$\gamma_{c,1}$	$\gamma_{c,2}$	$\gamma_{c,1}$	$\gamma_{c,2}$	$\gamma_{c,1}$	$\gamma_{c,2}$	$\gamma_{c,1}$	$\gamma_{c,2}$
cl\cl	−73.7306	−156.093	−72.8316	−155.152	−71.0303	−153.270	−67.4151	−149.499
cl\pn	−29.2847	−111.181	−28.5591	−110.267	−27.1055	−108.437	−24.1879	−104.771
cl\sl	−18.0303	−80.840	−17.1011	−79.793	−15.2323	−77.697	−11.4521	−73.500
cl\fr	−2.7775	−43.144	−2.0758	−42.148	−0.6639	−40.154	2.1959	−36.155
pn\cl	−51.3243	−127.962	−50.1425	−126.869	−47.7626	−124.682	−42.9348	−120.301
pn\pn	−17.6772	−85.315	−16.7810	−84.199	−14.9746	−81.961	−11.3021	−77.472
pn\sl	−6.3202	−54.479	−4.7683	−52.987	−1.5545	−50.021	5.3466	−44.191
pn\fr	1.0173	−24.139	2.0714	−22.645	4.3050	−19.682	9.3876	−13.957

Table 5
Rayleigh–Ritz $\gamma_{c,1}$ of *pn–pn* beam in Ref. [6] compared with 'exact' values

$\tau(0)$	0.0	−6.5	−41.5
$\gamma_{c,1}$ Ref. [6]	18.7	−6.5	83.0
$\gamma_{c,1}$ present	−18.56873	−6.59013	82.89464

Table 6
The first two critical $\tau(0)$ for various γ

BC	$\gamma = 10.0$		$\gamma = 4.0$		$\gamma = 1.0$		$\gamma = -1.0$	
O\A	$\tau_{c,1}(0)$	$\tau_{c,2}(0)$	$\tau_{c,1}(0)$	$\tau_{c,2}(0)$	$\tau_{c,1}(0)$	$\tau_{c,2}(0)$	$\tau_{c,1}(0)$	$\tau_{c,2}(0)$
cl\cl	−44.4390	−85.755	−41.4721	−82.762	−39.9780	−81.263	−38.9780	−80.263
cl\pn	−26.6628	−64.943	−22.7961	−61.784	−20.8441	−60.205	−19.5360	−59.154
cl\sl	−14.7601	−44.511	−11.8520	−41.484	−10.3685	−39.979	−9.3685	−38.979
cl\fr	−9.2673	−27.551	−5.2433	−24.314	−3.1679	−22.730	−1.7627	−21.685
pn\cl	−23.5849	−64.424	−21.5640	−61.577	−20.5360	−60.154	−19.8441	−59.205
pn\pn	−14.6983	−44.559	−11.8421	−41.491	−10.3679	−39.979	−9.3679	−38.979
pn\sl	−5.2486	−27.069	−3.6244	−24.132	−2.7626	−22.685	−2.1679	−21.730
pn\fr	−4.2182	−15.478	−1.8681	−11.974	−0.4916	−10.376	cc	−9.376
BC	$\gamma = -2.0$		$\gamma = -5.0$		$\gamma = -10.0$		$\gamma = -20.0$	
O\A	$\tau_{c,1}(0)$	$\tau_{c,2}(0)$	$\tau_{c,1}(0)$	$\tau_{c,2}(0)$	$\tau_{c,1}(0)$	$\tau_{c,2}(0)$	$\tau_{c,1}(0)$	$\tau_{c,2}(0)$
cl\cl	−38.4768	−79.763	−36.9685	−78.261	−34.4390	−75.755	−29.3207	−70.732
cl\pn	−18.8800	−58.628	−16.9040	−57.051	−13.5849	−54.424	−6.8540	−49.170
cl\sl	−8.8652	−38.480	−7.3422	−36.987	−4.7601	−34.511	0.5658	−29.606
cl\fr	−1.0539	−21.166	1.0960	−19.618	4.7514	−17.069	12.2918	−12.047
pn\cl	−19.4961	−58.731	−18.4440	−57.310	−16.6628	−54.943	−12.9928	−50.221
pn\pn	−8.8627	−38.482	−7.3267	−36.999	−4.6983	−34.559	0.8080	−29.792
pn\sl	−1.8641	−21.256	−0.9261	−19.847	0.7327	−17.551	4.4467	−13.192
pn\fr	1.0333	−8.896	2.7048	−7.531	5.7818	−5.478	12.7216	−1.892

Table 7
Approximate $\tau_{c,1}(0)$ of *pn–pn* beam in Ref. [14] compared with 'exact' values

γ	$-0.25\pi^2$	$-0.5\pi^2$	$-0.75\pi^2$	$-1.0\pi^2$	$-2.0\pi^2$	$-3.0\pi^2$
$\tau_{c,1}(0)$ Ref [14]	−8.63	−7.36	−6.08	−4.77	0.657	4.97
$\tau_{c,1}(0)$ present	−8.62544	7.36038	−6.07450	−0.76796	0.66028	6.39550

In Table 6 $\tau_{c,1}(0)$ and $\tau_{c,2}(0)$ pairing with $\gamma = 10, 4, 1, -1, -2, -5, -10$ and -20 are tabulated. The approximate $\tau_{c,1}(0)$ of $pn-pn$ beam for various values of γ obtained by Timoshenko and Gere [14] using one term Rayleigh method are compared with 'exact' values in Table 7. The accuracy of the approximate results for $\gamma > -2.0\pi^2$ is poor.

3. Concluding remarks

The system parameters of the title problem are the constant part of the axial force and the constant of proportionality of the varying component. The mode shape differential equation was solved by the method of Frobenius. The frequency equations were listed for 16 combinations of classical boundary conditions and the first three frequency parameters are tabulated for example combinations of system parameters. The effect of an increase in one or both of the system parameters was to cause an increase in the frequency parameter. Computations failed if the system parameters were large. This was due to the limitation on the 'precision' of the computing facility. Euler buckling occurs for the combination of the system parameters at which a frequency parameter is zero. A necessary (but not sufficient) condition for the onset of buckling is if one or both system parameters are negative. Example pairs of critical system parameters are tabulated. Some critical system parameter pairs obtained by Rayleigh–Ritz method are compared with "exact' values obtained by the analytical method.

The results tabulated may be used to judge frequencies and the buckling pairs of system parameters obtained by numerical methods.

Appendix A. Nomenclature

$a_{n+1}(c)$	coefficients in Eq. (5)
A, B	constants in Eq. (11)
c	exponent in Eq. (5)
D, D^n	$\mathrm{d}/\mathrm{d}X$, $\mathrm{d}^n/\mathrm{d}X^n$
$E(X), F(X)$, $G(X), H(X)$	solution functions of Eq. (10)
EI	flexural rigidity of beam
L	length of beam
m	mass per unit length of beam
$M(x)$	amplitude of bending moment
$Q(x)$	amplitude of shearing force
$M(X), Q(X)$	dimensionless bending moment, shearing force Eq. (3)
n	$= 0, 1, 2, \ldots \infty$
$T(x)$	axial force at abscissa x
$T(0), T(L)$	axial force at O and at A
$U(X), V(X)$	functions in Eq. (11)
x	abscissa
X	dimensionless abscissa Eq. (3)
$y(x)$	amplitude of beam deflection
$Y(X)$	dimensionless amplitude Eq. (3)
$Y(X, c)$	a solution Eq. (11)
α	frequency parameter Eq. (3)
γ	axial force variation parameter Eq. (3)
$\gamma_{c,1}, \gamma_{c,2}$	the first two critical γ

$\tau(X)$	dimensionless axial force
$\tau(0), \tau(1)$	dimensionless axial force at O and A
$\tau_{c,1}(0), \tau_{c,2}(0)$	the first two critical $\tau(0)$
α	frequency parameter Eq. (3)
ω	a natural frequency

References

[1] H. McCallion, *Vibration of Linear Mechanical Systems*, Longman, London, 1973.
[2] A. Bokaian, Natural frequencies of beams under compressive axial loads, *Journal of Sound and Vibration* 126 (1) (1988) 49–65.
[3] A. Bokaian, Natural frequencies of beams under tensile axial loads, *Journal of Sound and Vibration* 142 (3) (1990) 481–498.
[4] M.P. Païdoussis, P.E. Des Trois Maisons, Free vibration of a heavy, damped, vertical cantilever, *Transactions of the American Society of Mechanical Engineers, Journal of Applied Mechanics* 38 (1971) 524–526.
[5] B. Schafer, Free vibration of a gravity loaded clamped-free beam, *Ingenieur-Archiv* 55 (1985) 66–80.
[6] G. Fauconneau, W.M. Laird, Bounds for the natural frequencies of a simply supported beam carrying a uniformly distributed axial load, *Journal of Mechanical Engineering Science* 9 (2) (1967) 149–155.
[7] D.F. Pilkington, J.B. Carr, Vibration of beams subjected to end and axially distributed loading, *Journal of Mechanical Engineering Science* 12 (1) (1970) 70–72.
[8] T. Yokayama, Vibrations of a hanging Timoshenko beam under gravity, *Journal of Sound and Vibration* 141 (2) (1990) 245–258.
[9] S. Naguleswaran, Vibration of a vertical cantilever with and without axial freedom at clamped end, *Journal of Sound and Vibration* 146 (2) (1991) 191–198.
[10] F.B. Hildebrand, *Advanced Calculus for Applications*, 2nd Edition, Prentice Hall, Englewood Cliffs, NJ, 1976.
[11] A.G. Greenhill, Determination of the greatest height consistent with stability that a vertical pole or mast can be made and of the greatest height to which a tree of given proportions can grow, *Proceedings of the Cambridge Philosophical Society* 4 (1881) 65–73.
[12] R. Frish-Fay, The analysis of a vertical and a horizontal cantilever under a uniformly distributed load, *Journal of the Franklin Institute* 271 (1961) 192–199.
[13] S.D. Gooch, J.K. Raine, The dynamics and limits on the scaling of a flexible kinetic sculpture, *Proceedings of the Institution of Mechanical Engineers* 214 (Part C) (2000) 537–548.
[14] S.P. Timoshenko, J.M. Gere, *Theory of Elastic Stability*, 2nd Edition, McGraw-Hill, New York, 1963.